2021 43rd Annual International Conference of the
IEEE Engineering in Medicine & Biology Society (EMBC)
Oct 31 - Nov 4, 2021. Virtual Conference

A proof-of-concept study for the prediction of the de-novo atherosclerotic plaque development using finite elements*

Antonis I. Sakellarios, Panagiota Tsompou, Vassiliki Kigka, Gianna Karanasiou, Konstantina Tsarapatsani, Savvas Kyriakidis, Georgia Karanasiou, Panagiotis Siogkas, Sotiris Nikopoulos, Silvia Rocchiccioli, Gualtiero Pelosi, Lampros K. Michalis, Dimitrios I. Fotiadis, *Fellow, IEEE*

***Abstract*— The type of the atherosclerotic plaque has significant clinical meaning since plaque vulnerability depends on its type. In this work, we present a computational approach which predicts the development of new plaques in coronary arteries. More specifically, we employ a multi-level model which simulates the blood fluid dynamics, the lipoprotein transport and their accumulation in the arterial wall and the triggering of inflammation using convection-diffusion-reaction equations and in the final level, we estimate the plaque volume which causes the arterial wall thickening. The novelty of this work relies on the conceptual approach that using the information from 94 patients with computed tomography coronary angiography (CTCA) imaging at two time points we identify the correlation of the computational results with the real plaque components detected in CTCA. In the next step, we use these correlations to generate two types of de-novo plaques: calcified and non-calcified. Evaluation of the model's performance is achieved using eleven patients, who present de-novo plaques at the follow-up imaging. The results demonstrate that the computationally generated plaques are associated significantly with the real plaques indicating that the proposed approach could be used for the prediction of specific plaque type formation.**

Keywords: Plaque generation, finite elements, plaque growh.

I. Introduction

Coronary atherosclerosis is the most common form of the cardiovascular disease (CVD) responsible for the most yearly deaths worldwide [1]. Plaque vulnerability is a feature of the disease associated with major events, such as myocardial infarction (MI) or even death. It has been clinically found that lipidic plaques are more vulnerable than the calcified ones especially due to their difference in their elastic properties with the calcified plaques being stable and stiff enough against the hemodynamics forces.

Hemodynamics play a significant role in CVD. Though CVD is a systemic disease, hemodynamics is responsible for the local manifestations of the disease, where the endothelial shear stress (ESS) acts as a factor for alterations of the endothelial membrane functions in several levels e.g. biochemical and genetic, increasing its permeability to lipid components as well as triggering the inflammation at the regions of low ESS.

The effect of ESS on the pathophysiology of atherosclerosis was investigated in several computational studies [2]–[4]. The main outcome of these works was that low ESS is indeed associated with highest rates of disease progression. Subsequently, the low ESS has a negative effect to the endothelial physiology by increasing its permeability to low density lipoproteins (LDL) as demonstrated previously [5], [6]. A lot of effort was given previously from several researchers in the modelling of the mechanisms of atherosclerosis. In particular, a three level approach was proposed using proof or concept case studies or even idealized arterial geometries [7]–[10]. In these studies, the aim was to develop a computational model to simulate atherosclerotic plaque growth, assuming however, that the plaque is homogeneous. Very recently, Pleouras *et al*. [11] presented a novel computational model for plaque growth which employed 100 patients and it was validated using the follow-up imaging of these patients. This model predicts the formation of plaque and the arterial wall thickening with moderate accuracy.

In this work, we utilize this computational model as well as the clinical findings of the 100 patients to enhance the capabilities of the model to generate de-novo atherosclerotic plaques. For the first time, the generation of plaques is performed in real human data and a proof-of-concept demonstration of the model's effectiveness is demonstrated using real follow-up imaging. Since the development of this model was based on CTCA imaging, we assume that calcified and non-calcified plaques can be generated. This was done in order to validate the computational findings with the CTCA imaging data. Data from eleven patients with de-novo plaques at the follow-up time point were used to validate the current model.

*This work is partially funded by the European Commission: Project InSilc: In-silico trials for drug-eluting BVS design, development and evaluation (GA number: 777119).

A. Sakellarios, S. Kyriakidis, G. Karanasiou and D.I. Fotiadis are with the Dept. of Biomedical Research, FORTH-IMBB, GR 45110 Ioannina, Greece (corresponding author phone: +302651009006; fax: +302651008889; e-mail: fotiadis@uoi.gr).

A. Sakellarios, P.K. Siogkas, P. Tsompou, V. Kigka, K. Tsarapatsani and D.I. Fotiadis are with the Unit of Medical Technology and Intelligent Information Systems, Department of Materials Science and Engineering, University of Ioannina, Ioannina, GR 45110 Greece.

S. Rocchiccioli and G. Pelosi are with Institute of Clinical Physiology, National Research Council, 56124, Pisa, Italy (email: pelosi@ifc.cnr.it).

S. Nikopoulos and L. K. Michalis is with the Dept. of Cardiology, Medical School, University of Ioannina, Ioannina, GR 45110, Greece.

II. Material and Methods

A. Population

During the H2020 SMARTool project (Clinicaltrial.gov Identifiers NCT04448691) [12], a prospective, multicenter study was conducted. Ethical approval was provided by each participating center (National Research Council, Italy, University of Turku, Finland, University of Zurich, Switzerland, Fondazione Toscana Gabriele Monasterio, Italy, Warsaw National Institute of Cardiology, Poland) through the approval of the clinical study by the Ethics Committee Vast Area Northwest of Tuscany (CEAVNO), Pisa, Italy, and all subjects gave written informed consent. The clinical study follows the declaration of Helsinki [11]. 94 patients were selected from this population, for which clinical information as well as CTCA imaging was available at least at two time points for analysis and used for plaque growth simulation. From these 94 patients, a sub-class of eleven patients was chosen where plaques could be identified only on the follow-up CTCA scans constituting de-novo plaques, which would be used for the validation of the presented study.

B. CTCA analysis and 3D reconstruction

The 3D reconstruction of both the baseline and follow-up CTCA imaging was performed using an in house 3D reconstruction and plaque characterization tool [13], [14], which provided the lumen area, the plaque volume and the plaque burden. An overview of the methodology can be summarized in the pre-processing of the images, resulting in the removal of the blooming effect of the calcified plaques, the identification of the potential vessel regions, the segmentation, and 3D plaque reconstruction which is achieved using a 3D level set algorithm. An arterial example is shown in Fig. 1. The methodology is able to segment and provide 3D reconstructions of the calcified and non-calcified plaques.

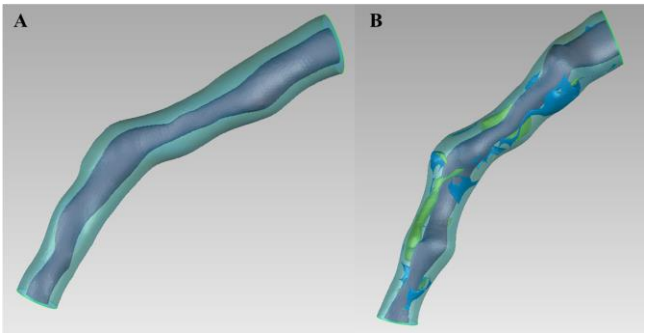

Figure 1. A case example of the baseline (left) and the follow-up (right) coronary arterial 3D reconstruction with calcified (yellow) and non-calcified plaques (blue).

C. Plaque growth simulation

In this step, simulation of plaque growth was performed in a sub-population of the eleven patients. Patient-specific parameter values were utilized for the LDL, high density lipoprotein (HDL) and pressure and were applied as boundary conditions. The model was previously validated for its effectiveness to simulate the disease progression in terms of plaque growth. Briefly, in the first level of the model, blood flow is simulated employing the Navier-Stokes equations to assess the ESS distribution on the endothelial membrane. The ESS values are used as input for the simulation of plaque growth and its major biological and biochemical processes as a second level. These include: i) the LDL, HDL and monocytes transport and penetration through the endothelial membrane in the arterial wall, ii) the oxidation of LDL particles considering the athero-protective effect of HDL, iii) the inflammation triggering through the appearance of macrophages, iv) the formation of foam cells, v) the presence of collagen and proliferation of smooth muscle cells. These processes are simulated employing convection-diffusion-reaction equations. In the final level, the total plaque volume is estimated by the sum of the smooth muscle cells, foam cells and collagen concentrations and it is used to simulate the thickening of the arterial wall causing the lumen narrowing.

D. De-novo plaque generation

The methodology for the generation of the *de-novo* plaques is based on the results of the previous section. The simulation results (ESS, LDL concentration, HDL concentration, oxidized LDL concentration, monocytes, macrophages, collagen, foam cells, SMCs) were extracted in 0.5mm cross-sections as well as to 3mm arterial segments. Using the 3mm values of all plaque growth modelling variables, their mean values for each coronary segment are calculated. In parallel, for each coronary arterial segment, the information regarding the calcified and non-calcified plaque count and volume, from the 3D reconstruction and plaque characterization tool are used.

In the next step, the correlations between the plaque growth modelling variables and the calcified and non-calcified plaque volumes per artery are identified. For the correlated variables, a ROC curve analysis was performed to identify the threshold over which calcified or non-calcified plaque should be generated based on the associated computational variable. At the final stage, we assume that the nodes of the finite element mesh correspond to calcified or non-calcified plaque according to the nodal variables' values. In case of values lower than the defined thresholds, we assume that there is normal tissue of arterial wall. The overall methodology is presented in Fig. 2. The identified statistically significant correlations after the analysis of the abovementioned populations are between the monocytes and calcified plaque and between the SMCs and the non-calcified plaque volume. The ROC curve (AUC=0.685, P=0.025) between the monocyte and the calcified plaques is presented in Fig. 3, while the ROC curve (AUC=0.615, P=0.042) between the SMCs and the non-calcified plaque is shown in Fig. 4. The thresholds were extracted based on the ROC curve. In particular, when SMCs concentration is over 37,641 cells/m^3, the mesh nodes were classified as non-calcified plaque. When monocytes were over $2.34*10^{10}$ cells/m^3, the nodes were classified as calcified plaque. In all other regions, normal tissue was assumed. In all other regions, normal tissue was assumed.

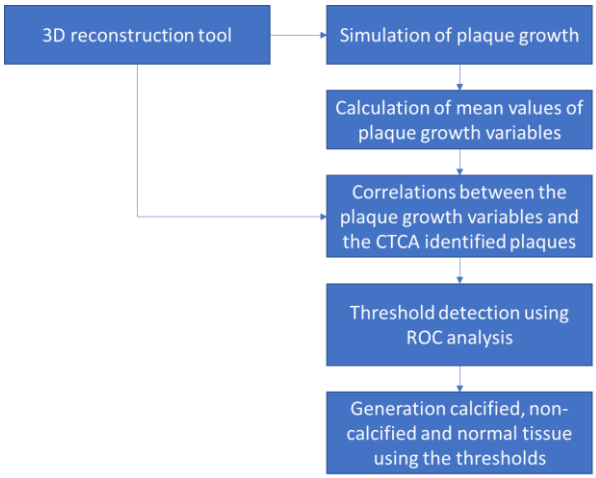

Figure 2. The methodology to generate de-novo plaques.

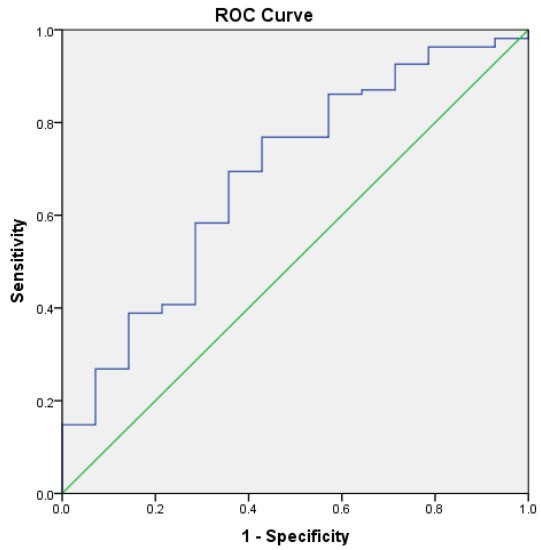

Figure 3. ROC curve between the monocytes and the calcified plaque volume.

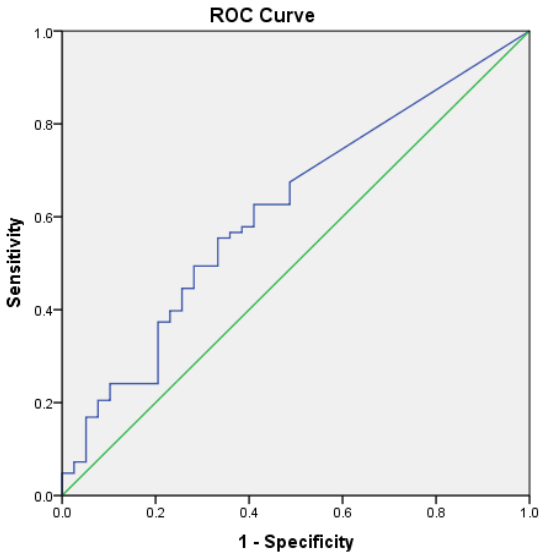

Figure 4. ROC curve between the SMCs and the non-calcified plaque volume.

III. Results

Using the above mentioned methodology we performed plaque growth simulations using the baseline arterial geometries and we produced de-novo calcified and non-calcified plaques. An example of generated plaque geometries is presented in Fig. 5. which shows a direct comparison between the simulated generated calcified plaque and the realistic follow-up reconstructed geometries of lumen and calcified plaque after the simulation using the real follow-up period of 7 years. There is good visual agreement especially for the largest object of the calcified plaque.

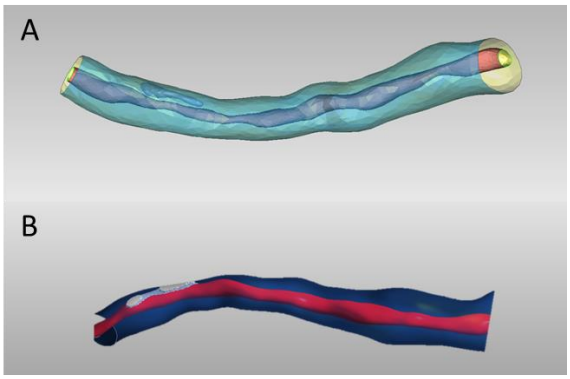

Figure 5. A: Follow-up geometry where the calcified plaque is present (blue) distributed to the whole arterial wall, B: The produced calcified plaque (white) after the simulation. Good agreement is found on the volume of the generated plaque.

Figure 6 presents a right coronary artery, in which non-calcified plaque was detected in the follow-up CTCA images. The plaque is found at the inner side of the curve, as well as at the proximal part of the arterial segment. The simulation of the plaque growth model produced only non-calcified plaques. In particular, two major non-calcified plaques were detected, both located at the same location as the real reconstructed plaques.

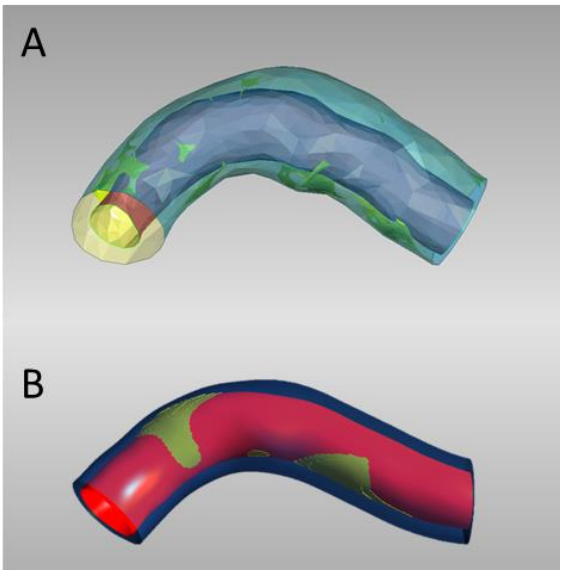

Figure 6. A: The real follow-up geometry based on the CTCA imaging where the non-calcified plaque is present (yellow), B: The produced non-calcified plaque after the simulation. Good agreement is found on the location of the generated plaque.

We also examine the correlation of the simulated findings (degree of stenosis, minimum lumen diameter and lesion length) with the real findings at the follow-up CTCA imaging, where good agreement is observed (Fig. 7).

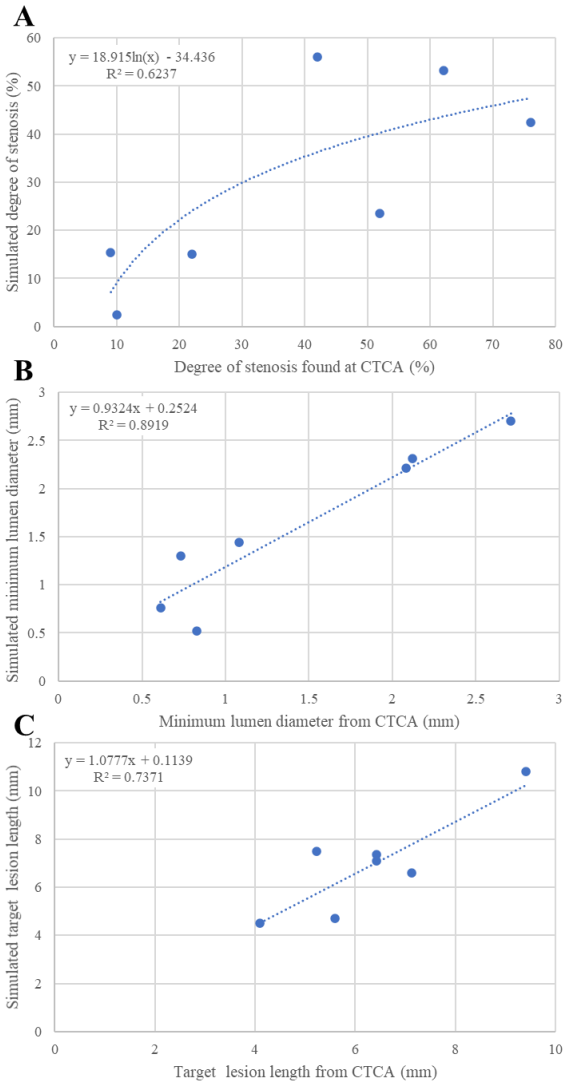

Figure 7. Correlation of degree of stenosis, minimum lumen diameter and lesion length for the simulated findings with the real follow-up at CTCA.

IV. Discussion and Conclusions

In this work, we present a novel approach for the generation of de-novo calcified and non-calcified plaques. This is based on computational simulation of plaque growth using a multi-level model of the major atherosclerotic disease processes. Such as model has significant clinical meaning, as it could be used for preventive or prognostic strategies. In particular, plaque destabilization is affected by several biological and biomechanical factors such including the ESS and the blood flow forces acting on the arterial wall. Vulnerable plaques are characterized by cap thickness <65 μm [15], large necrotic core and increased macrophage infiltration. However, these could not easily be detected using non-invasive imaging, such as the CTCA. Using the proposed model, it could be possible to predict the vulnerable plaques non-invasively and propose an accurate approach for the management of the disease.

The limitation of the current approach is its employment in as small dataset of eleven patients. However, we aim to further validate the current model using additional patients with non-invasive imaging as well as patients with invasive imaging where detailed analysis of the plaque composition is possible.

References

[1] World Health Organization (WHO), "The atlas of heart disease and stroke." http://www.who.int/cardiovascular_diseases/en/cvd_atlas_16_death_from_stroke.pdf.

[2] A. Sakellarios *et al.*, "The effect of coronary bifurcation and haemodynamics in prediction of atherosclerotic plaque development: a serial computed tomographic coronary angiographic study," *EuroIntervention*, vol. 13, no. 9, pp. e1084–e1091, Oct. 2017, doi: 10.4244/EIJ-D-16-00929.

[3] C. V. Bourantas *et al.*, "Implications of the local haemodynamic forces on the phenotype of coronary plaques," *Heart*, vol. 105, no. 14, pp. 1078–1086, Jul. 2019, doi: 10.1136/heartjnl-2018-314086.

[4] P. H. Stone *et al.*, "Role of Low Endothelial Shear Stress and Plaque Characteristics in the Prediction of Nonculprit Major Adverse Cardiac Events: The PROSPECT Study," *JACC Cardiovasc Imaging*, Sep. 2017, doi: 10.1016/j.jcmg.2017.01.031.

[5] A. Sakellarios *et al.*, "Prediction of atherosclerotic disease progression using LDL transport modelling: a serial computed tomographic coronary angiographic study," *European heart journal cardiovascular Imaging*, Mar. 2016, doi: 10.1093/ehjci/jew035.

[6] A. I. Sakellarios *et al.*, "Patient-specific computational modeling of subendothelial LDL accumulation in a stenosed right coronary artery: effect of hemodynamic and biological factors," *Am J Physiol-Heart C*, vol. 304, no. 11, pp. H1455–H1470, Jun. 2013, doi: 10.1152/ajpheart.00539.2012.

[7] A. Sakellarios *et al.*, "Prediction of Atherosclerotic Plaque Development in an in Vivo Coronary Arterial Segment Based on a Multi-level Modeling Approach," *IEEE transactions on bio-medical engineering*, Oct. 2016, doi: 10.1109/TBME.2016.2619489.

[8] P. Siogkas *et al.*, "Multiscale - Patient-Specific Artery and Atherogenesis Models," *Ieee T Bio-Med Eng*, vol. 58, no. 12, pp. 3464–3468, Dec. 2011, doi: 10.1109/Tbme.2011.2164919.

[9] V. Calvez Houot, J. G. ,. Meunier, N. ,. Raoult, A. ,. Rusnakova, G., "Mathematical and numerical modeling of early atherosclerotic lesions," 2010, vol. 30, pp. 1–14.

[10] M. Cilla, E. Pena, and M. A. Martinez, "Mathematical modelling of atheroma plaque formation and development in coronary arteries," *J R Soc Interface*, vol. 11, no. 90, Jan. 2014, doi: 10.1098/Rsif.2013.0866.

[11] D. S. Pleouras *et al.*, "Simulation of atherosclerotic plaque growth using computational biomechanics and patient-specific data," *Scientific Reports*, vol. 10, no. 1, Art. no. 1, Oct. 2020, doi: 10.1038/s41598-020-74583-y.

[12] Smit Jeff M. *et al.*, "Impact of Clinical Characteristics and Statins on Coronary Plaque Progression by Serial Computed Tomography Angiography," *Circulation: Cardiovascular Imaging*, vol. 13, no. 3, p. e009750, Mar. 2020, doi: 10.1161/CIRCIMAGING.119.009750.

[13] V. I. Kigka *et al.*, "3D reconstruction of coronary arteries and atherosclerotic plaques based on computed tomography angiography images," *Biomedical Signal Processing and Control*, vol. 40, pp. 286–294, Feb. 2018, doi: 10.1016/j.bspc.2017.09.009.

[14] V. I. Kigka *et al.*, "A three-dimensional quantification of calcified and non-calcified plaques in coronary arteries based on computed tomography coronary angiography images: Comparison with expert's annotations and virtual histology intravascular ultrasound," *Computers in Biology and Medicine*, vol. 113, p. 103409, Oct. 2019, doi: 10.1016/j.compbiomed.2019.103409.

[15] A. P. Burke, A. Farb, G. T. Malcom, Y. Liang, J. Smialek, and R. Virmani, "Coronary Risk Factors and Plaque Morphology in Men with Coronary Disease Who Died Suddenly," *New England Journal of Medicine*, vol. 336, no. 18, pp. 1276–1282, May 1997, doi: 10.1056/NEJM199705013361802.